Geophysical Research Letters

RESEARCH LETTER
10.1029/2023GL103902

The Relationship Between the Present-Day Seasonal Cycles of Clouds in the Mid-Latitudes and Cloud-Radiative Feedback

K. Furtado[1,2], Y. Tsushima[1], P. R. Field[1,3], J. Rostron[1], and D. Sexton[1]

[1]Met Office Hadley Centre, Exeter, UK, [2]Now at Centre for Climate Research Singapore (CCRS), Meteorological Service Singapore, National Environment Agency (NEA), Singapore, Singapore, [3]School of Earth and Environment, University of Leeds, Leeds, UK

Key Points:

- Seasonal cycles of clouds constrain cloud feedbacks
- The northern ocean basins are natural laboratories for low-cloud feedbacks
- The hot-model problem in HadGEM3 will not easily be solved by tuning

Supporting Information:

Supporting Information may be found in the online version of this article.

Correspondence to:

K. Furtado,
kalli_furtado@nea.gov.sg

Citation:

Furtado, K., Tsushima, Y., Field, P. R., Rostron, J., & Sexton, D. (2023). The relationship between the present-day seasonal cycles of clouds in the mid-latitudes and cloud-radiative feedback. *Geophysical Research Letters*, *50*, e2023GL103902. https://doi.org/10.1029/2023GL103902

Received 31 MAR 2023
Accepted 8 JUN 2023

Author Contributions:

Conceptualization: K. Furtado
Data curation: J. Rostron, D. Sexton
Investigation: K. Furtado
Methodology: K. Furtado, Y. Tsushima, P. R. Field
Software: K. Furtado
Validation: K. Furtado
Writing – original draft: K. Furtado
Writing – review & editing: Y. Tsushima, P. R. Field

Abstract We show that the seasonal cycles of clouds over the mid-latitude oceans in the Northern Hemisphere are predictors of the responses of clouds to increasing sea-surface temperatures globally. These regions are therefore "natural laboratories" in which the processes responsible for low-cloud feedbacks on global scales are observed as seasonal changes in local cloud properties. We use an ensemble of configurations of a global-climate model to show that the sensitivities of cloud-radiative anomalies to surface temperature and lower-tropospheric stability in the "laboratory" regions predict the models' global cloud-radiative feedbacks. Models with greater changes in low-clouds between seasons are shown to have stronger negative feedbacks in the mid-latitudes, and stronger positive feedbacks from the subtropical stratocumulus. The biases in the simulated seasonal cycles, compared to observations, imply that both feedbacks are too weak in the model. The consequences of this for configuring our model to have a lower climate sensitivity are discussed.

Plain Language Summary As the Earth's climate warms, feedbacks from changes in clouds are crucial for determining the rate of warming. In some climate models, positive cloud feedbacks are known to contribute to projected temperature increases which fall outside the range that is considered plausible given our current understanding of the Earth's climate. Methods are needed which directly relate present-day model errors to projected cloud feedbacks so that we can understand how to improve models and simultaneously obtain plausible feedback strengths. We show that in the Met Office Hadley Centres' climate model, the seasonal cycles of clouds in a few key regions, specifically the poleward ocean basins in the Northern Hemisphere, can be used to predict cloud feedbacks, globally, across a wide range of configurations of the model. These regions, particularly the North-west Pacific, are "natural laboratories" in which the same processes that are responsible for global, cloud-feedbacks onto global-warming rates, occur annually as part of the local seasonal cycle. Studying clouds in these regions and model biases in predictions of these clouds will allow us to directly improve estimates of global climate change.

1. Introduction

The response of the Earth's globally averaged temperature to radiative forcing agents is the most fundamental quantity in climate-change prediction. Many of the uncertainties in current best-estimates are due uncertainties in feedbacks, within the climate system, which either enhance or reduce the temperature changes due to the direct effect of a radiative forcing. Feedbacks due to changes in clouds are particularly uncertain because the instrumental record of cloud observations is short, and current theoretical understanding of the mechanisms remains ambiguous.

Recently, a paradigm of "cloud-controlling factors" has been shown to be useful for reducing the uncertainty in cloud feedbacks (Ceppi & Nowack, 2021). This approach is based on the long-standing observation that a relatively small number of environmental factors exert a substantial level of control over cloud properties (Klein & Hartmann, 1992). Amongst these properties surface temperature and lower-tropospheric stability are known to be particularly useful for understanding the variability of clouds across a broad range of time- and spatial-scales. Ceppi and Nowack (2021) showed that the sensitivities of cloud properties to changes in these factors can be used to estimate future changes in cloud-radiative effects (CREs), under the assumption that the sensitivities themselves are stable in time (i.e., that they are not strongly altered by radiative forcing; an assumption i.e., supported by available evidence from numerical modeling). Hence, it appears that present-day natural variability in clouds and cloud-controlling factors, can be used to obtain observationally-based estimates of future changes in clouds

as a result of a forcing. This in turn can be used to assess the plausibility of the climate sensitivities of individual numerical models.

Two time-scales that can be expected to feature prominently in any analysis of variations in clouds and their controlling factor are the seasonal cycle and inter-annual variability (Klein & Hartmann, 1992). The former may be very pronounced at mid- or high-latitudes, where both temperature and stability change by many degrees between summer and winter. Moreover, because seasonal variations are responses to the annual cycle of incoming solar radiation it can be hypothesized that the seasonal cycle in cloud properties may contain information about how clouds will respond to other types of forcing (such as atmospheric concentrations of greenhouse gases). This has led us, in a previous paper, to consider in detail the seasonal cycles of CREs over the northwestern Pacific, where the seasonal cycles of cloud-controlling factors are particularly large (Furtado & Tsushima, 2023). Our study revealed biases in the responses of CREs to the seasonal cycles of temperature and stability in an ensemble of atmosphere-only climate simulations, and identified the cloud regimes and simulated processes that were most responsible for the biases. Viewed from within the cloud-controlling factor paradigm, these biases in responses should be analogous to biases in cloud feedbacks to global warming. For example, models with more biased present-day seasonal cycles may be those with less plausible cloud-radiative feedbacks (CRFs) and if so, then there should be a correlation between seasonal-cycle biases and cloud feedbacks.

Met Office Hadley Centres' HadGEM3 family of global-climate models (Hewitt et al., 2011) have been shown to project climate sensitivities which at the high end of multi-model estimates (Andrews et al., 2019), when compared with other models that participated in the Climate Model Intercomparison Project Phase 6 (CMIP6). Moreover, the sensitivities of the HadGEM3 models are known to be outside of range that is considered plausible based on many collaborating pieces of evidence, including estimates based on cloud-controlling factor (Sherwood et al., 2020). This is despite the HadGEM3 models consistently being amongst the most successful prediction systems, when evaluated for many aspects of model performance for present-day climate (Williams et al., 2017). Indeed, because of the Met Office's "seamless" approach to weather and climate services, members of same family are routinely shown to be highly capable of providing operational forecasts on all time-scales from hours to decades ahead. This seeming conflict between good present-day performance, and a climate sensitivity that is not commensurate with current best-estimates, suggests a deep-rooted structural deficiency in the modeling system, and has called into question its use for studying climate changes (Hausfather et al., 2022).

It is also known that the climate sensitivity of the latest generations of the HadGEM family, HadGEM3 Global Coupled version 3 (GC3) and later, are greater than those of preceding generations. This was traced in part of improvements in the simulation of cloud cover and cloud-hydrometeor phase in post-frontal (cold sector) conditions in the wakes of mid-latitude cyclones (Bodas-Salcedo et al., 2016), which improved longstanding biases in top-of-atmosphere (TOA) radiant fluxes and near-surface temperatures over the Southern Ocean (Hyder et al., 2018). A lack of supercooled liquid water in these clouds was a long-standing model bias, prior to GC3, which was addressed by a package of changes to the parametrizations of clouds and aerosols (Bodas-Salcedo et al., 2019). These improvements increased the CRF in the mid-latitudes, since conversion of ice to liquid clouds causes a strongly negative shortwave-radiative feedback as the temperature warms because liquid droplets are more reflective of sunlight than ice crystals of the same mass (Tsushima et al., 2006). This so-called "mixed-phase feedback" has an overall cooling effect on the atmosphere, so its mitigation was detrimental for the global-mean radiative feedback, because a potent negative feedback mechanism was weakened. This was despite the present-day climatologies of mid-latitude clouds being improved, especially over the Southern Ocean (Furtado et al., 2016), suggesting that either the Southern Ocean was improved via a physically incorrect approach, or cloud biases there were compensating for other biases elsewhere, or there is another negative cloud-feedback mechanism over the Southern Ocean that is poorly represented Mülmenstädt et al. (2021).

In this study, we use a Perturbed Parameter Ensemble (PPE) of the atmosphere-land component of HadGEM3-GC to identify regions where the present-day seasonal cycles of CREs correlate with the CRFs calculated from experiments with a fixed-spatial pattern of sea-surface temperature (SST) perturbations. The ensemble is constructed by perturbing parameters in the model's physics schemes, in a way that samples their perceived uncertainties and thereby generates a large range of historical climates (Sexton et al., 2019). By comparing the feedbacks from the ensemble members with the feedback estimated using observations of the present-day seasonal cycles of CREs and cloud-controlling factors, we show that the ensemble systematically *underestimates* the magnitude of the negative low-cloud feedback over the Southern Ocean, and simultaneously underestimates a positive feedback

from the subtropical stratocumulus. This will allow us to suggest that, without novel and structural changes to the model's physics, aimed at decoupling the physical processes which influence mid-latitude, mixed-phase clouds and subtropical, warm clouds, it will be difficult to configure HadGEM3 to have a substantially lower cloud feedback and therefore a smaller climate sensitivity.

2. Global Cloud Feedbacks and the Local Seasonal Cycle

Our PPE is 500 configurations of the HadGEM3 Global Atmosphere and Land version 8 (GAL8), obtained by perturbing 71 parameters from the model's cloud, radiation, turbulence and land-surface schemes in a way that samples prior estimates of parameter uncertainty that were solicited from the developers of the schemes (Sexton et al., 2019, 2021). For each configuration, two atm-land only experiments were run: a 5-year integration, following the Atmosphere Model Inter-comparison Project (AMIP) protocol, using historical SSTs; and a 5-year AMIPFuture experiment with a patterned SST, corresponding to 4K of sea-surface warming globally (Webb et al., 2017). Such experiments are known to provide good estimates of cloud feedbacks from coupled-climate projections (Ringer et al., 2014). Differencing a CRE between this pair of experiments for each member and dividing by temperature increments provides a canonical way of defining the CRF, at each grid-point, for that radiation component, that is, the CRF due to changes in a CRE is defined as $\Lambda = \Delta\text{CRE}/\Delta T_S$, where T_S is the local surface temperature, and we use a proceeding Δ to indicate differences in quantities between the AMIP and AMIPFuture simulations. Because not all the AMIP simulations give reasonable estimates of historical TOA fluxes, we restrict our analysis to ensemble members with global-mean net absolute TOA-flux errors within ± 2 Wm^{-2} of the observational estimate from the Clouds and the Earth's Radiant Energy System (CERES) Energy Balanced and Filled 1-degree Synoptic (SYN1deg) TOA and surface fluxes and clouds product (Loeb et al., 2018).

We will consider two cloud-controlling factors, the surface temperature (T_S) and a measure of lower-tropospheric stability called the Estimated Inversion Strength (EIS) which is defined following the recipe given in Wood and Bretherton (2006). From previous studies, these two factors are known to be related to natural variability in CREs on a range of scales. For a given controlling factor, X, we will be interested in the linear responses of cloud properties, y (e.g., CREs), to changes in X. We will call these responses the cloud-response functions, $G_y(X) = \delta y/\delta X$, where we use a δ to indicate the change in a quantity between two different atmospheric states in the historical simulations (a difference between two different months, for example).

The response functions measure the sensitivity of cloud properties to local changes in the controlling factors. Furtado and Tsushima (2023) used the average seasonal cycles of clouds and cloud-controlling factors in the Oyashio region (139–191°E, 42–54°N), in the north-western Pacific, to quantify the response functions of CREs and cloud-area fractions. Two aspects of the seasonal cycle in the Oyashio make it particularly amenable to controlling-factor analysis: first, its mid-latitude location results in large-amplitude seasonal cycles of SST and EIS; second, the climatological seasonal cycles of SST and EIS are lagged in time relative to each other by approximately 3 months. This later property implies that the minimum of SST occurs at a time of year when EIS is increasing and the EIS-maximum occurs when the surface is warming. The time-lag between control factors provides a convenient way of partitioning the globe into regions which are internally coherent in terms of seasonal variations in SST and EIS. Therefore, for this study we generalize our analysis of the Oyashio to use the seasonal cycles at all locations where the phase difference between SST and EIS is between 2 and 4 months. Decomposition of the ensemble-mean seasonal cycle of monthly means into Fourier modes was used to define the phase of each control factor. The global map of phase differences in Figure 1a shows that the targeted 2–4-month lags are mainly found in the North Pacific, the North Atlantic and along a narrow band around the edge of the Southern Ocean. Over land and over the tropical oceans the seasonal cycles are closer to ± 6 months out-of-phase, indicating that in those places surface temperature and stability peak in opposite seasons. We will restrict attention to the parts of the phase-lagged region that lie in the Northern Hemisphere, and denote this region by $\mathcal{D}_{\text{lag}}$. Clouds in this region experience similar variations of controlling factors throughout the year. The mean seasonal cycles of SST and EIS in $\mathcal{D}_{\text{lag}}$ are shown in Figure 1b, for the PPE members (blue shading), the PPE-ensemble mean (blue line) and the European Centre for Medium-range Weather Forecasts Reanalysis version 5 (ERA5) (black).

Associated with seasonal cycles in the cloud-controlling factors, we find large seasonal variations in CREs and clouds fractions in $\mathcal{D}_{\text{lag}}$. Radiative effects are conveniently quantified by radiant-flux anomalies due to the presence of clouds, normalized by the incoming solar flux at the top of the atmosphere. The seasonal cycle of the normalized SW CRE, R_s, is shown in Figure 1c (we use the subscript s for "shortwave"). The observational

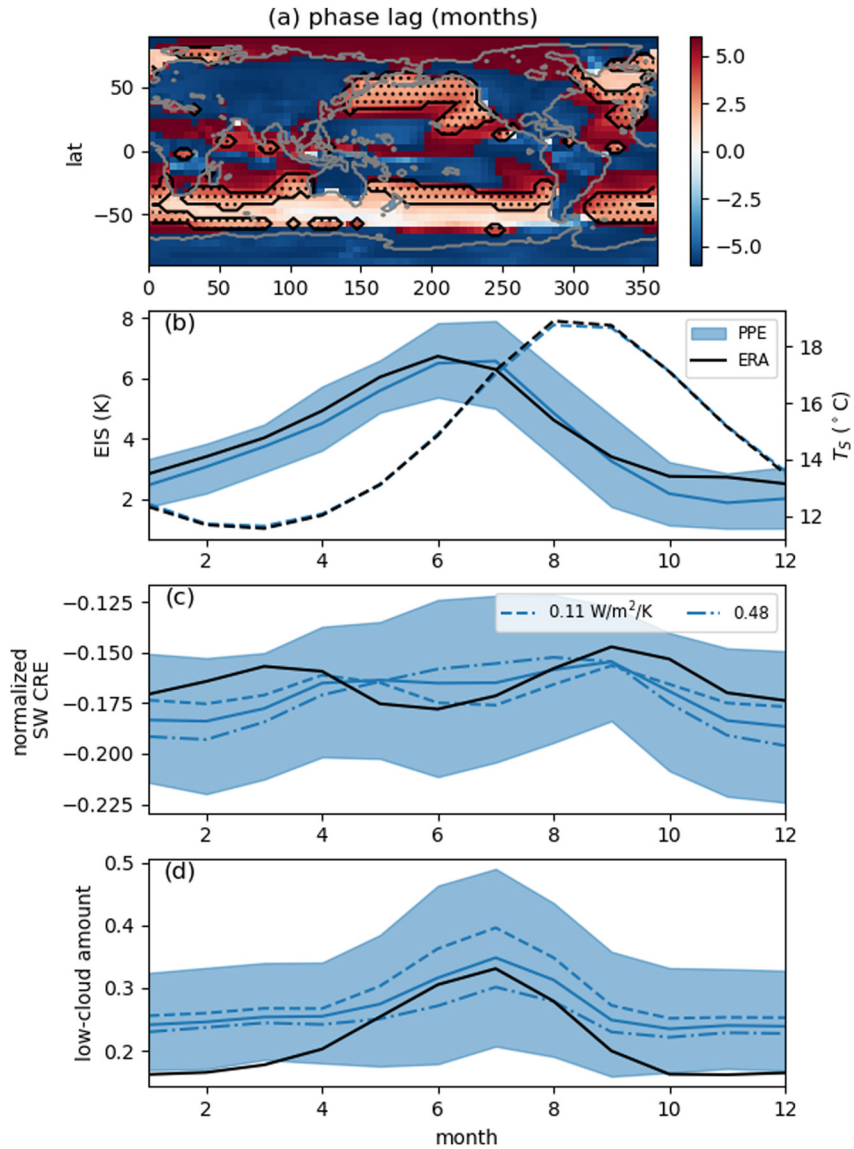

Figure 1. (a) Phase lag between the seasonal cycles of T_S and Estimated Inversion Strength (EIS) for the Perturbed Parameter Ensemble (PPE). The black-dotted contour shows a phase lag of 2 months. (b) The average cycles of EIS (solid) and T_S (dashed) in the region (D_{lag}) with 2–4 month lags, for PPE (blue) and ERA5 (black). PPE range is shaded blue. (c) Cycle on D_{lag} of the normalized SW cloud-radiative effect for CERES-EBAF (black) and PPE. The averages of PPE-members in the bottom- and top-deciles of net cloud-radiative feedback are the dashed and dot-dashed lines. (d) The cycle of thick and medium-thick low cloud in International Satellite Cloud Climatology Project (black) and PPE.

estimate of the real seasonal cycle obtained from CERES-EBAF is shown by the black line. The observations have a double-peak structure, with local minima in both June and December. The PPE members produce a range of seasonal cycles, which can resemble the observations more or less closely, depending on the parameter settings of each configuration. A first indication that there is a close relationship between global-mean CRFs, and the local seasonal cycle in D_{lag} is given by the decorated blue lines in Figure 1c. To obtain these we stratify the seasonal cycle according to the feedback in the global-mean of the non-normalized net CRE, r_n, which is denoted by $\overline{\Lambda}_n = \overline{\Delta r_n / \Delta T_S}$ (using the above notation), where $\overline{(\cdot)}$ denotes a global mean and we use the subscript n for "net." The lines show the mean seasonal cycles of the members with $\overline{\Lambda}_n$ in the lowest (dashed line) top-most (dot-dashed line) deciles of the PPE. (Note that the numerical values in legend in Figure 1c are the ensemble-mean values of $\overline{\Lambda}_n$ in the two deciles.) We see that the models with weaker (less positive) net CRFs have seasonal cycles that are more similar to the satellite retrievals than for those members with stronger (more positive) feedbacks. In

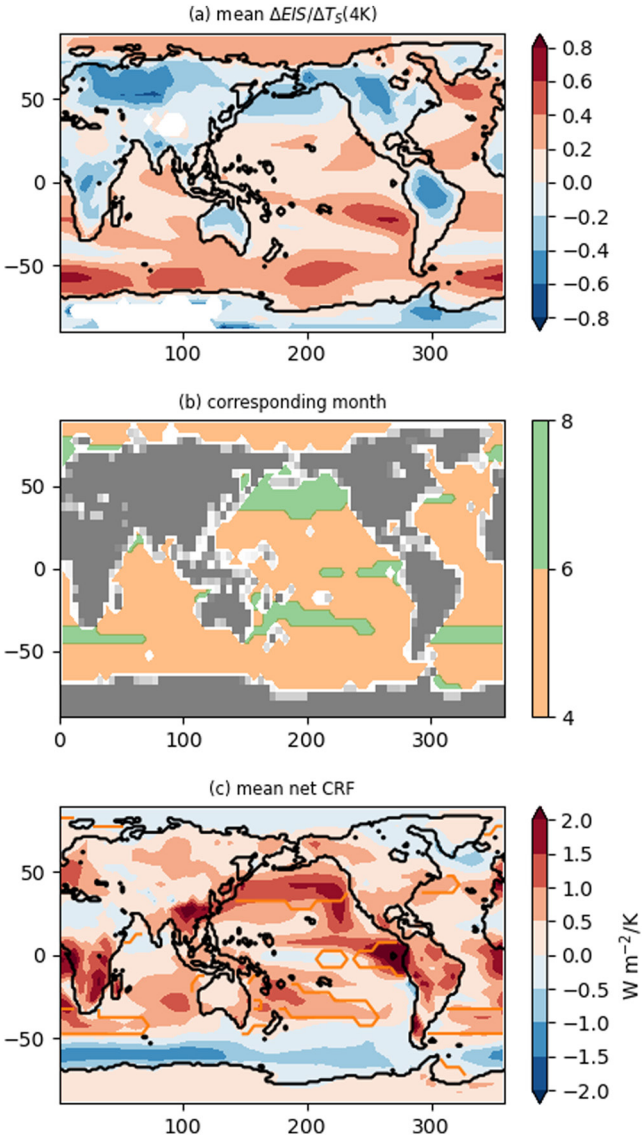

Figure 2. (a) The PPE-mean change in Estimated Inversion Strength (EIS) per unit local temperature change between the Atmosphere Model Inter-comparison Project (AMIP) and AMIPFuture experiments for each member. (b) The month of the year for which the rate-of-change in EIS with temperature during the seasonal cycle on the phase-lagged region is closest to $\Delta\text{EIS}/\Delta T_S$ each point. (c) The PPE-mean net cloud-radiative feedback. The orange contour shows the boundary between the regions corresponding to May and July.

particular, we note that weak-feedback models are better able to represent the decrease in R_s that occurs from April to June. By contrast, strong-feedback configurations have normalized SW CREs that continue to increase throughout the summer, which is less realistic when compared to CERES-EBAF.

In the Oyashio region, the main driver of SW CRE tendencies in early summer (e.g., from May to July) is the amount of optically thick low cloud (Furtado & Tsushima, 2023). This is also true for the whole of $\mathcal{D}_{\text{lag}}$, as can be seen from Figure 1d which shows the seasonal cycle of the fractional area covered by clouds that are at low-levels (i.e., have tops at atmospheric pressures greater than 680 hPa) and have medium or thick optical depths according to the classification of the International Satellite Cloud Climatology Project (ISCCP) (Rossow & Schiffer, 1999). In the observations, the low-thick cloud fraction, φ, is least in winter and increases during spring to attain a maximum in mid-summer. The PPE members systematically overestimate winter-time cloud, but span the ISCCP observations in summer, when some members overestimate low-cloud amount whilst others underestimate it. Hence there is substantial inter-member spread in the rates of increase of φ during spring. Stratification of the low-cloud cycles into deciles of net CRF shows that this spread is closely related to the cloud feedbacks and the summer-time SW CRE: models in the top-most decile of $\overline{\Lambda}_n$ are those for which low-cloud increases most rapidly in spring and are associated with the most rapid rates of deepening of R_s.

The seasonal cycle in $\mathcal{D}_{\text{lag}}$ samples a range of monthly increments in the controlling-factors, T_S and EIS, and cloud properties, for example, R_s, φ, etc. For any month, m_0 (May($m_0 = 5$), for example), there are increments, $\delta T_S = T_S(m_0 + 1) - T_S(m_0 - 1)$, etc., and corresponding CRE-response functions $G_s(T_S) = \delta R_s/\delta T_S$ and $G_s(\text{EIS}) = \delta R_s/\delta\text{EIS}$. Similarly, the global map of the ensemble-mean changes in EIS between the AMIP and AMIPFuture simulations in Figure 2a shows that the geographical distribution of the sensitivity, $\Lambda_{\text{EIS}} = \Delta\text{EIS}/\Delta T_S$, of EIS to T_S also samples a range of values, depending on location. To relate inter-model differences in the seasonal cycle of SW CRE in $\mathcal{D}_{\text{lag}}$ to CRFs at other locations, we identify each model configuration and grid point with a corresponding month, m_0, for which the EIS change, Λ_{EIS}, due to AMIPFuture SSTs, is closest to the observed $G^{\text{obs}}_{\text{EIS}}(T_S) = \delta\text{EIS}/\delta T_S$ calculated from ERA5 for the interval (m_0 − 1, m_0 + 1) of the seasonal cycle in the phase-lagged region. Hence for any model configuration (PPE member), r, and any point, p, on the globe, there is a month of the year $m_0(r, p)$ when the observed change in EIS with surface temperature in $\mathcal{D}_{\text{lag}}$, at that time, is most similar to the simulated change in EIS with global-SST warming for configuration r at p. Our assumption is that cloud responses during the seasonal cycle in $\mathcal{D}_{\text{lag}}$, at that time of year, are indicative of the cloud changes due to global-SST warming at the point in question (which may be remote from the phase-lagged region), because low-cloud cloud changes induced by global warming may be controlled by changes in EIS and T_S. If this assumption holds, it indicates that cloud-property changes during the seasonal cycle in D_{lag} are influenced by the same physical processes which affect cloud changes due to global warming, perhaps because the prevalent cloud regimes are the similar in both case. The assumption is, of course, not likely to hold for regions such as the deep tropics where the dominant regimes differ substantially from those in D_{lag}. For such regions, an approach linking variability and feedbacks at the same location, such as was introduced by Ceppi and Nowack (2021), may be needed. Figure 2b shows a map of the modal corresponding month at each point, globally. (Recall that each ensemble has it own corresponding month for each grid point, so we define modal month to be the month shared by more than 50% of the ensemble members.) At most ocean points the EIS-response to SST can be associated with the increase in EIS for May in $\mathcal{D}_{\text{lag}}$. Exceptions are the mid-latitude ocean basins, particularly in the North Pacific, where the EIS feedback is better represented by EIS changes in July.

We are interested in the relationships between the seasonal SW CRE responses to controlling factors, $G_s(T_S)$ and G_s(EIS), in the corresponding month, and the net CRF, Λ_n, at each point. The relationships between Λ_n and the G_ss will be statistically easier to identify at points where there are substantial changes in SW CRE due to global-SST warming. Figure 2c shows that these points are mostly located in the region corresponding to a modal month of May. In particular, the PPE simulates a large positive net feedback over the subtropical stratocumulus and a large negative feedback and over the Southern Ocean. These are therefore regions where we expect any correlations between feedbacks and responses to be largest. To quantify these correlations we use multi-linear, least squares regression of cloud feedbacks onto $G_s(T_S)$ and G_s(EIS) for the corresponding month (considering only May, since this accounts for most locations globally). For each cloud property, α (e.g., a CRE or cloud fraction), this approach yields a linear model for the cloud feedback, Λ_α, in terms of the seasonal responses of SW CRE to T_S and EIS in the phase-lagged region in the corresponding month, where the regression coefficients depend on latitude and longitude. By calculating the response functions from the CERES-EBAF retrievals of SW CRE, we can obtain an observationally constrained estimate of the feedback by substituting the observed responses into the linear predictor.

The relationships between the responses functions and the net CRF can be seen in Figure 3a which shows the correlations between Λ_s and $G_s(T_S)$. The response function is positively correlated with the feedback over the Southern Ocean, indicating that weakening the sensitivity of normalized SW CRE to SST in $\mathcal{D}_{\text{lag}}$ (i.e., making the rate of decrease of R_s with temperature less negative in May) is associated with weakening the negative cloud-feedback over the Southern Ocean. Or, equivalently, that ensemble members with more realistic (i.e., more rapidly decreasing) seasonal changes in SW CRE in the phase-lagged region, have more strongly negative net CRFs over the Southern Ocean. The opposite effect is seen over the subtropical stratocumulus regions, where strengthening the sensitivity of SW CRE to T_S leads to an increase in the strength of a positive cloud-feedback.

Figure 3b shows the differences between the ensemble-mean net CRF and the observational estimate obtained by calculating the response functions from CERES-EBAF and substituting these into the linear regression obtained from the PPE. We see that the PPE systematically overestimates the feedback over the Southern Ocean and North Atlantic, and underestimates the feedback over the subtropical stratocumulus in the North-east Pacific. The overestimated mid-latitude feedback occurs because, on average, the PPE predicts a net CRF that is not as strongly negative as the observations suggest. Whereas the underestimated subtropical feedback occurs because the positive net CRF is too weak in this region. These biases in net CRF are associated with the biases in the low-cloud amount feedback, Λ_φ, that are shown in Figure 3c. Low-cloud fraction over the Southern Ocean increases less strongly that the observations suggest, and decreases too weakly in the subtropics. Hence, the excessively weak negative CRFs in the mid-latitudes are associated with insufficient increases in low-cloud cover, whilst the excessively weak positive CRFs in the subtropics are linked to smaller-than-observed reductions in cloud cover.

The relationships between the cloud-response function, $G_s(T_S)$, and the net CRF over the Southern Ocean and subtropical stratocumulus are shown in Figure 4a, which compares the area-averaged net CRFs with the R_s response to temperature averaged over $\mathcal{D}_{\text{lag}}$, for each PPE member (colored points). The vertical black line shows the response calculated from CERES-EBAF, and the black dots show the observationally estimated net CRFs for each region. We see that almost all the PPE members have responses that are too large compared to the observations. For the stratocumulus region (orange points), selecting model parameters which reduce the response function bias will typically result in a stronger positive feedback. Similarly, improving the response function will give a model with a more negative net feedback over the Southern Ocean (blue points). The biases in these two regions account for almost all of the bias in the global-mean net CRF, $\overline{\Lambda}_n$. However, because of the opposite signs of the biases in the two regions, they approximately cancel each other out globally (Figure 4b), resulting in a weakly reducing global-mean net CRF in response to improving the historical seasonal cycle.

3. Discussion and Implications for Model Developments

An important characteristic of the current generation of the HadGEM3 family of climate models is their high climate sensitivities, which are outside the range that some studies suggest is plausible. At least part of model's high climate sensitivity is known to arise from CRFs, so proposing methods of controlling these is a pressing concern. Our results suggest that improving the representation of the seasonal cycle in northern ocean basins, particular then north-western Pacific, can give a physically justified way of reducing the net CRF, and therefore also the climate sensitivity. Central to this claim is the residual negative correlation between the globally

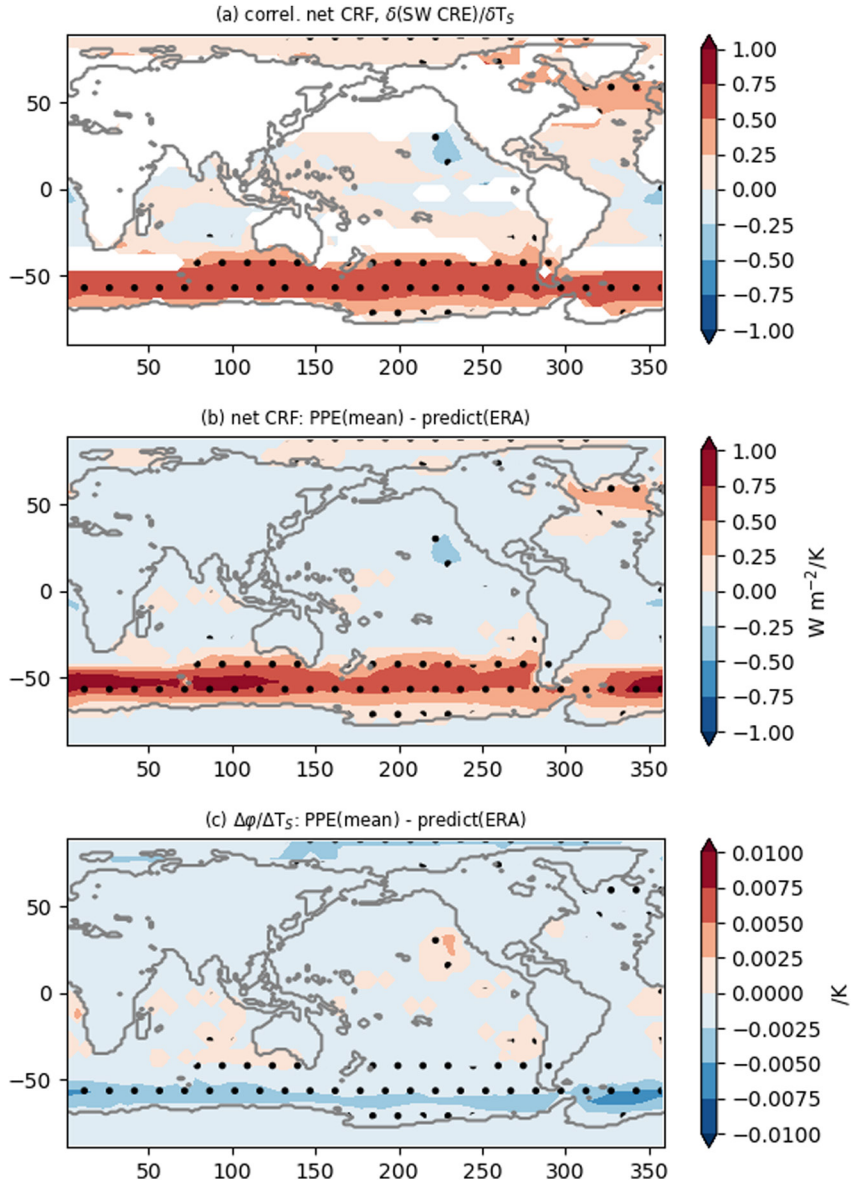

Figure 3. (a) Correlation coefficient between net cloud-radiative feedback (CRF) and the SW CRE-response to T_S. (b) The bias in the PPE-mean net CRF, compared to the linear estimator evaluated on the observed values of the SW CRE-response functions. (b) The bias in the PPE-mean low-thick cloud amount, compared to the linear estimator. The dots indicate correlation significance below 0.01, using a Student's *t*-test.

averaged net CRF, $\overline{\Lambda}_n$, and seasonal response of SW CRE, $G_s(T_S)$, shown in Figure 4b, which occurs because a negative CRF from increasing low-cloud amount in the mid-latitudes dominates over a positive feedback due to reductions in subtropical cloud amount. This indicates that the only *systematic* route to configuring HadGEM3 to have a lower net CRF, that is explored within the PPE, is to enhance the negative Southern Ocean feedback. This is in keeping with the finding of Mülmenstädt et al. (2021) that the CMIP6 models underestimate the strength of a negative cloud fraction feedback over the Southern Ocean, despite significant improvements to the thermodynamic phase of such clouds compared to CMIP5. It is therefore possible that the seasonal cycle mainly constrains the cloud-fraction component of the feedback, and is relatively uninformative of the cloud-phase feedback proposed by Tsushima et al. (2006), and others. This suggestion is also consistent with the prevalence of warm (liquid only) clouds in the $\mathcal{D}_{\text{lag}}$ region in summer (Kawai et al., 2015). Therefore, future work to identify common mechanisms for the seasonal cycle in $\mathcal{D}_{\text{lag}}$ and Southern Ocean feedbacks may give information on the relative importance of different feedbacks.

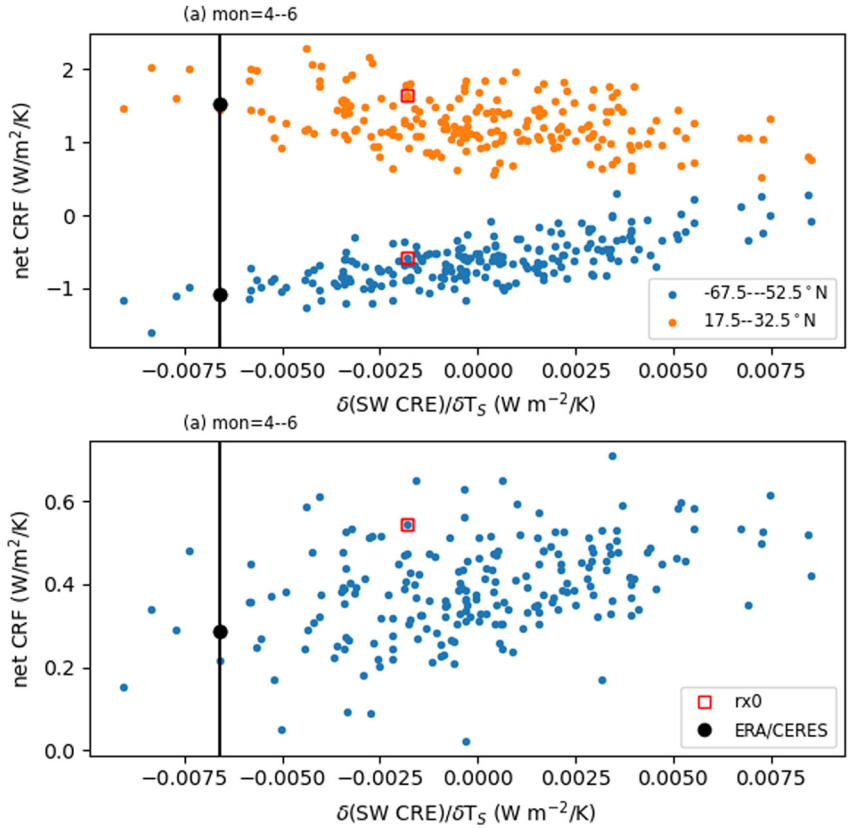

Figure 4. Relationships between the SW CRE-responses to temperatures and net cloud-radiative feedback (CRF) averaged over: (a) the subtropical stratocumulus region (orange) and the Southern Ocean (blue); (b) the entire globe. The vertical black lines are the observed values of the response functions. The black points are net CRFs linearly estimated from the observations. The red squares show the locations of GAL8. The correlation coefficients are −0.38, 0.72, and 0.40 for the stratocumulus region, Southern Ocean and globe, respectively.

Because a strengthening of the negative feedback over the Southern Ocean is accompanied by an opposing tendency for the subtropical feedback to become more positive, the overall sensitivity of the models net CRF to improving the cloud-response functions is relative weak. In addition, modifying the model parameters to reduce the positive feedback in the subtropics is, first, not consistent with the observational constraint from the historical seasonal cycle and, second, results in a compensatory weakening the mid-latitude feedback which dominates over the subtropics and leads to more positive feedback globally.

This coupled "subtropical–midlatitude" mode of inter-model variability emerges as the leading-order relationship in our analysis of responses to cloud-controlling factors based on the seasonal cycle alone. However, the scatter in the points in Figures 4a and 4b indicates that the PPE does explore behaviors that are not systematically related to the response functions considered here. These indicate parameter sensitivities which would permit lower feedbacks to be explored, without necessarily degrading the contemporary seasonal cycle. In this respect, it is interesting to note the biases in the default-model configuration (GAL8, itself), which are shown by the red-squares in Figures 4a and 4b. This model has an adequate seasonal cycle (it is not in the worst performing 50% of models for the response metric), but it has net CRFs in both regions that are larger than would be expected from the linear regression alone. There are therefore parameter changes which reduce the net CRF in GAL8 without substantially changing cloud-response functions. The effects of these parameters changes may be related to other aspects of present-day, observable model-performance, and in particular to cloud-response functions that are not related to the seasonal cycle in D_{lag}. This will be investigated by us in a later publication.

Data Availability Statement

The data supporting the conclusions of this paper can be obtained from https://doi.org/10.5281/zenodo.7789574.

Acknowledgments
Funding for this research was provide by the UK-China Research and Innovation Partnership Fund through the Met Office Climate Science for Service Partnership China as part of the Newton Fund.

References

Andrews, T., Andrews, M. B., Bodas-Salcedo, A., Jones, G. S., Kuhlbrodt, T., Manners, J., et al. (2019). Forcings, feedbacks, and climate sensitivity in HadGEM3-GC3.1 and UKESM1. *Journal of Advances in Modeling Earth Systems*, *11*(12), 4377–4394. https://doi.org/10.1029/2019ms001866

Bodas-Salcedo, A., Hill, P. G., Furtado, K., Williams, K. D., Field, P. R., Manners, J. C., et al. (2016). Large contribution of supercooled liquid clouds to the solar radiation budget of the Southern Ocean. *Journal of Climate*, *21*(11), 4213–4228. https://doi.org/10.1175/jcli-d-15-0564.1

Bodas-Salcedo, A., Mulcahy, J. P., Andrews, T., Williams, K. D., Ringer, M. A., Field, P. R., & Elsaesser, G. S. (2019). Strong dependence of atmospheric feedbacks on mixed-phase microphysics and aerosol-cloud interactions in HadGEM3. *Journal of Advances in Modeling Earth Systems*, *11*(6), 1942–2466. https://doi.org/10.1029/2019ms001688

Ceppi, P., & Nowack, P. (2021). Observational evidence that cloud feedback amplifies global warming. *Proceedings of the National Academy of Sciences USA*, *118*(30), 25–43. https://doi.org/10.1073/pnas.2026290118

Furtado, K., Field, P. R., Boutle, I. R., Morcrette, C. J., & Wilkinson, J. M. (2016). A physically-based, subgrid parametrization for the production and maintenance of mixed-phase clouds in a general circulation model. *Journal of the Atmospheric Sciences*, *73*(1), 279–291. https://doi.org/10.1175/jas-d-15-0021.1

Furtado, K., & Tsushima, Y. (2023). Simulations of the seasonality of clouds in the northwestern Pacific with an ensemble of climate–model configurations. *Journal of the Meteorological Society of Japan*, *11*, 1–1.

Hausfather, Z., Marvel, K., Schmidt, G. A., Nielsen-Gammon, J. W., & Zelinka, M. (2022). Climate simulations: Recognize the 'hot model' problem. *Nature*, *605*(7908), 26–29. https://doi.org/10.1038/d41586-022-01192-2

Hewitt, H. T., Copsey, D., Culverwell, I. D., Harris, C. M., Hill, R. S. R., Keen, A. B., et al. (2011). Design and implementation of the infrastructure of HadGEM3: The next-generation Met Office climate modelling system. *Geoscientific Model Development*, *4*(2), 223–253. https://doi.org/10.5194/gmd-4-223-2011

Hyder, P., Edwards, J. M., Allan, R. P., Hewitt, H. T., Bracegirdle, T. J., Gregory, J. M., et al. (2018). Critical Southern Ocean climate model biases traced to atmospheric model cloud errors. *Nature Communications*, *8*(1), 3625. https://doi.org/10.1038/s41467-018-05634-2

Kawai, H., Yabu, S., Hagihara, Y., Koshiro, T., & Okamoto, H. (2015). Characteristics of the cloud top heights of marine boundary layer clouds and the frequency of marine fog over mid-latitudes. *Journal of the Meteorological Society of Japan. Ser. II*, *93*(6), 613–628. https://doi.org/10.2151/jmsj.2015-045

Klein, S. A., & Hartmann, D. L. (1992). The seasonal cycle of low stratiform clouds. *Journal of Climate*, *6*(8), 1587–1606. https://doi.org/10.1175/1520-0442(1993)006<1587:tscols>2.0.co;2

Loeb, N. G., Doelling, D. R., Wang, H., Su, W., Nguyen, C., Corbett, J. G., et al. (2018). Clouds and the earth's radiant energy system (CERES) energy balanced and filled (EBAF) top-of-atmosphere (TOA) edition-4.0 data product. *Journal of Climate*, *31*(2), 895–918. https://doi.org/10.1175/JCLI-D-17-0208.1

Mülmenstädt, J., Salzmann, M., Kay, J. E., Zelinka, M. D., Ma, P. L., Nam, C., et al. (2021). An underestimated negative cloud feedback from cloud lifetime changes. *Nature Climate Change*, *11*(6), 508–513. https://doi.org/10.1038/s41558-021-01038-1

Ringer, M. A., Andrews, T., & Webb, M. J. (2014). Global-mean radiative feedbacks and forcing in atmosphere-only and coupled atmosphere-ocean climate change experiments. *Geophysical Research Letters*, *41*(11), 4035–4042. https://doi.org/10.1002/2014gl060347

Rossow, W. B., & Schiffer, R. A. (1999). Advances in understanding clouds from ISCCP. *Bulletin of the American Meteorological Society*, *80*(11), 2261–2288. https://doi.org/10.1175/1520-0477(1999)080<2261:aiucfi>2.0.co;2

Sexton, D. M. H., Karmalkar, A. V., Murphy, J. M., Williams, K. D., Boutle, I. A., Morcrette, C. J., et al. (2019). Finding plausible and diverse variants of a climate model. Part 1: Establishing the relationship between errors at weather and climate time scales. *Climate Dynamics*, *53*(1–2), 989–1022. https://doi.org/10.1007/s00382-019-04625-3

Sexton, D. M. H., McSweeney, C. F., Rostron, J. W., Yamazaki, K., Booth, B. B., Murphy, J. M., et al. (2021). A perturbed parameter ensemble of HadGEM3-GC3.05 coupled model projections: Part 1: Selecting the parameter combinations. *Climate Dynamics*, *56*(11–12), 3395–3436. https://doi.org/10.1007/s00382-021-05709-9

Sherwood, S. C., Webb, M. J., Annan, J. D., Armour, K. C., Forster, P. M., Hargreaves, J. C., et al. (2020). An assessment of earth's climate sensitivity using multiple lines of evidence. *Reviews of Geophysics*, *58*(4), e2019RG000678. https://doi.org/10.1029/2019rg000678

Tsushima, Y., Emori, S., Ogura, T., Kimoto, M., Webb, M. J., Williams, K. D., et al. (2006). Importance of the mixed-phase cloud distribution in the control climate for assessing the response of clouds to carbon dioxide increase: A multi-model study. *Climate Dynamics*, *27*(2–3), 113–126. https://doi.org/10.1007/s00382-006-0127-7

Webb, M. J., Andrews, T., Bodas-Salcedo, A., Bony, S., Bretherton, C. S., Chadwick, R., et al. (2017). The cloud feedback model intercomparison project (CFMIP) contribution to CMIP6. *Geoscientific Model Development*, *10*(1), 359–384. https://doi.org/10.5194/gmd-10-359-2017

Williams, K. D., Copsey, D., Blockley, E. W., Bodas-Salcedo, A., Calvert, D., Comer, R., et al. (2017). The Met Office global coupled model 3.0 and 3.1 (GC3.0 and GC3.1) configurations. *Journal of Advances in Modeling Earth Systems*, *10*(2), 357–380. https://doi.org/10.1002/2017ms001115

Wood, R., & Bretherton, C. S. (2006). On the relationship between stratiform low cloud cover and lower-tropospheric stability. *Journal of Climate*, *19*(24), 6425–6432. https://doi.org/10.1175/jcli3988.1

References From the Supporting Information

Best, M. J., Pryor, M., Clark, D. B., Rooney, G. G., Essery, R., Ménard, C. B., et al. (2021). The Joint UK Land Environment Simulator (JULES), model description – Part 1: Energy and water fluxes. *Geoscientific Model Development*, *4*(3), 677–699. https://doi.org/10.5194/gmd-4-677-2011

Furtado, K., & Field, P. (2017). The role of ice microphysics parametrizations in determining the prevalence of supercooled liquid water in high-resolution simulations of a Southern Ocean midlatitude cyclone. *Journal of the Atmospheric Sciences*, *74*(6), 2001–2021. https://doi.org/10.1175/JAS-D-16-0165.1

Liu, Y., Daum, P. H., Guo, H., & Peng, Y. (2008). Dispersion bias, dispersion effect, and the aerosol-cloud conundrum. *Environmental Research Letters*, *3*(4), 045021. https://doi.org/10.1088/1748-9326/3/4/045021

Sexton, D. M. H., McSweeney, C. F., Rostron, J. W., Yamazaki, K., Booth, B. B. B., Murphy, J. M., et al. (2021). A perturbed parameter ensemble of HadGEM3-GC3.05 coupled model projections: Part 1: Selecting the parameter combinations. *Climate Dynamics*, *56*(11–12), 3395–3436. https://doi.org/10.1007/s00382-021-05709-9

Walters, D., Baran, A. J., Boutle, I., Brooks, M., Earnshaw, P., Edwards, J., et al. (2019). The Met Office Unified Model global atmosphere 7.0/7.1 and JULES global land 7.0 configurations. *Geoscientific Model Development*, *12*(5), 1909–1963. https://doi.org/10.5194/gmd-12-1909-2019